

A Native Ternary Complex Trapped in a Crystal Reveals the Catalytic Mechanism of a Retaining Glycosyltransferase**

David Albasa-Jové, Fernanda Mendoza, Ane Rodrigo-Unzueta, Fernando Gomollón-Bel, Javier O. Cifuentes, Saioa Urresti, Natalia Comino, Hansel Gómez, Javier Romero-García, José M. Lluch, Enea Sancho-Vaello, Xevi Biarnés, Antoni Planas, Pedro Merino, Laura Masgrau, and Marcelo E. Guerin*

Abstract: Glycosyltransferases (GTs) comprise a prominent family of enzymes that play critical roles in a variety of cellular processes, including cell signaling, cell development, and host–pathogen interactions. Glycosyl transfer can proceed with either inversion or retention of the anomeric configuration with respect to the reaction substrates and products. The elucidation of the catalytic mechanism of retaining GTs remains a major challenge. A native ternary complex of a GT in a productive mode for catalysis is reported, that of the retaining glucosyl-3-phosphoglycerate synthase GpgS from *M. tuberculosis* in the presence of the sugar donor UDP-Glc, the acceptor substrate phosphoglycerate, and the divalent cation cofactor. Through a combination of structural, chemical, enzymatic, molecular dynamics, and quantum-mechanics/molecular-mechanics (QM/MM) calculations, the catalytic mechanism was unraveled, thereby providing a strong experimental support for a front-side substrate-assisted S_Ni -type reaction.

Glycosyltransferases (GTs) play a central role in nature. GTs catalyze the transfer of a sugar moiety from nucleotide-sugar or lipid-phospho-sugar donors to a wide range of acceptor substrates, including mono-, oligo-, and polysaccharides, lipids, proteins, small organic molecules, and nucleic acids.^[1,2] As a consequence, GTs generate a significant amount of structural diversity in biological systems, which is

particularly apparent in the maintenance of the structural integrity of the cell in the modulation of molecular recognition events, including cell signaling, cell–cell communication, and cell–pathogen interactions.^[3] GTs can be classified as either ‘inverting’ or ‘retaining’ enzymes according to the anomeric configuration of the reaction substrates and products (Figure S1 in the Supporting Information).^[1] The reaction mechanism of inverting GTs seems to follow a single-displacement mechanism with an oxocarbenium ion like transition state and an asynchronous S_N2 mechanism, analogous to that observed for inverting glycosyl hydrolases.^[1] By contrast, the catalytic mechanism for retaining GTs is currently a matter of strong debate. By analogy with glycosyl hydrolases, a double displacement mechanism via the formation of a covalent glycosyl-enzyme intermediate was first suggested. Such a mechanism would involve an enzymatic nucleophile positioned within the active site on the β -face of the donor substrate in close proximity to the anomeric reaction center (Figure 1 A). Supporting this notion, chemical rescue of the mammalian α -(1→3)-galactosyltransferase Glu317Ala mutant by sodium azide has been reported.^[4] More recently, molecular dynamics simulations and density functional theory (DFT) Quantum Mechanics/Molecular Mechanics (QM/MM) calculations have also confirmed the formation of a covalent glycosyl-enzyme intermediate in the

[*] Dr. D. Albasa-Jové, A. Rodrigo-Unzueta, Dr. J. O. Cifuentes, Dr. S. Urresti, N. Comino, Dr. E. Sancho-Vaello, Prof. M. E. Guerin Unidad de Biofísica, Consejo Superior de Investigaciones Científicas - Universidad del País Vasco/Euskal Herriko Unibertsitatea (CSIC-UPV/EHU) and Departamento de Bioquímica, Universidad del País Vasco

48940 Leioa, Bizkaia (Spain)
E-mail: mrcguerin@gmail.com

Dr. L. Masgrau
Institut de Biociències i de Biomedicina (IBB) (Spain)

F. Mendoza, Prof. J. M. Lluch
IBB and Departament de Química
Universitat Autònoma de Barcelona, 08193 Bellaterra (Spain)

Dr. H. Gómez
IBB and Joint BSC-CRG-IRB Program in Computational Biology
IRB Barcelona, 08028 Barcelona (Spain)

F. Gomollón-Bel, Prof. P. Merino
Laboratorio de Síntesis Asimétrica, Departamento de Síntesis y Estructura de Biomoléculas, Instituto de Síntesis Química y Catálisis Homogénea (ISQCH), Universidad de Zaragoza, CSIC 50009 Zaragoza, Aragón (Spain)

J. Romero-García, Dr. X. Biarnés, Prof. A. Planas
Laboratory of Biochemistry, Institut Químic de Sarrià
Universitat Ramon Llull, 08017 Barcelona (Spain)
Dr. D. Albasa-Jové, Prof. M. E. Guerin
IKERBASQUE, 48013 Bilbao (Spain)

[**] This work was supported by the EU Contract HEALTH-F3-2011-260872, MINECO Contract BIO2013-49022-C2-2-R, and the Basque Government (to M.E.G.); MINECO Contracts CTQ2011-24292 and CTQ2014-53144-P (to J.M.LL.) and “UAB - Banco Santander Program” (to L.M.); CTQ2013-44367-C2-1-P (to P.M.) and MINECO Contract BIO2013-49022-C2-1-R (to A.P.). We acknowledge Diamond Light Source (proposals mx8302/10130), Soleil (proposal 20140843), and BioStruct-X (proposals 2460/5594/7687) for providing access to synchrotron radiation facilities. We gratefully acknowledge S. López-Fernández and P. Arrasate (Unit of Biophysics, CSIC, UPV/EHU, Spain), E. Ogando and T. Mercero (Scientific Computing Service UPV/EHU, Spain) for technical assistance. F.G.-B. and F.M. acknowledge support from the JAE Predoc Program (CSIC) and “Becas de Doctorado en el Extranjero - Becas Chile - CONICYT” Program, respectively.

Supporting information for this article is available on the WWW under <http://dx.doi.org/10.1002/anie.201504617>.

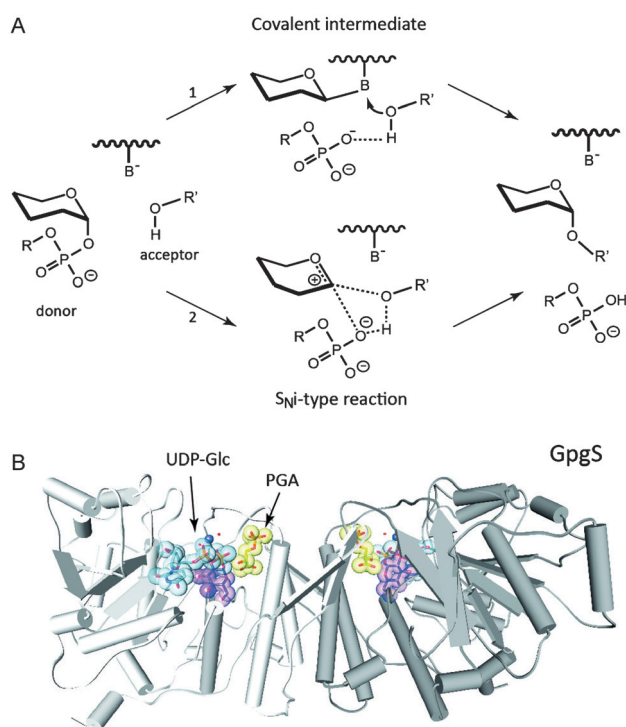


Figure 1. A) Proposed catalytic mechanisms for enzymatic glycosyl transfer with retention of the anomeric configuration: a double displacement mechanism (1) and a front-face mechanism (2). B) Overall structure of GpgS in complex with UDP-Glc, PGA, and the Mn^{2+} cofactor.

enzyme.^[5–7] Covalent intermediates have also been detected for the human blood group synthesizing α -(1 \rightarrow 3)-*N*-acetyl-galactosaminyltransferase (GTA) and α -(1 \rightarrow 3)-galactosyl-transferase (GTB) mutants by mass spectrometry.^[8,9] However, in the absence of a residue near the reaction center that can act as a nucleophile to form the glycosyl-enzyme intermediate, an alternative mechanism known as the $\text{S}_{\text{N}}\text{i}$ ‘internal return’, also called the $\text{S}_{\text{N}}\text{i}$ -like mechanism, has been suggested (Figure 1A).^[11,10–12] In this mechanism, leaving group departure and nucleophilic attack occur on the same face of the sugar^[13] and involve either a short-lived oxocarbenium ion intermediate ($\text{S}_{\text{N}}\text{i}$ -like)^[6,9,14–16] or an oxocarbenium ion transition state ($\text{S}_{\text{N}}\text{i}$).^[17]

To further advance the understanding of the catalytic mechanism of retaining glycosyl transfer reactions, we investigated the glucosyl-3-phosphoglycerate synthase (GpgS) from *Mycobacterium tuberculosis*. GpgS is a retaining glucosyltransferase that initiates the biosynthetic pathway of 6-*O*-methylglucose lipopolysaccharides (MGLPs) in mycobacteria, by transferring a glucose (Glc) moiety from uridine diphosphate (UDP)-Glc to the 2 position of the phosphoglycerate (PGA) to form glucosyl-3-phosphoglycerate (Figure 1B and Figure S2).^[18,19] As with most of the members of the GT-A superfamily of GTs, GpgS uses a divalent cation as an essential cofactor for enzymatic activity. Kinetic studies have demonstrated that the enzyme prefers Mg^{2+} for maximal activity in vitro. However, GpgS was less but still enzymatically active when another group II metal ion (Ca^{2+}) or transition metal ions (Mn^{2+} , Co^{2+} , or Fe^{2+}) were introduced

in the reaction mixture.^[18] The strategy for capturing a native ternary complex $\text{GpgS}\cdot\text{Mn}^{2+}\cdot\text{UDP-Glc}\cdot\text{PGA}$ was to carry out quick-soak experiments of unliganded GpgS crystals with the sugar donor UDP-Glc and acceptor substrate PGA in the presence of Mn^{2+} at different time points. We thus obtained three snapshots of the reaction center at resolutions of 2.3 Å, 2.3 Å, and 2.6 Å, thereby providing for the first time the atomic coordinates of a native Michaelis complex for a GT in the absence of any substrate derivative or protein mutant (Figure 2 and Table S1 and Figure S5 in the Supporting Information).

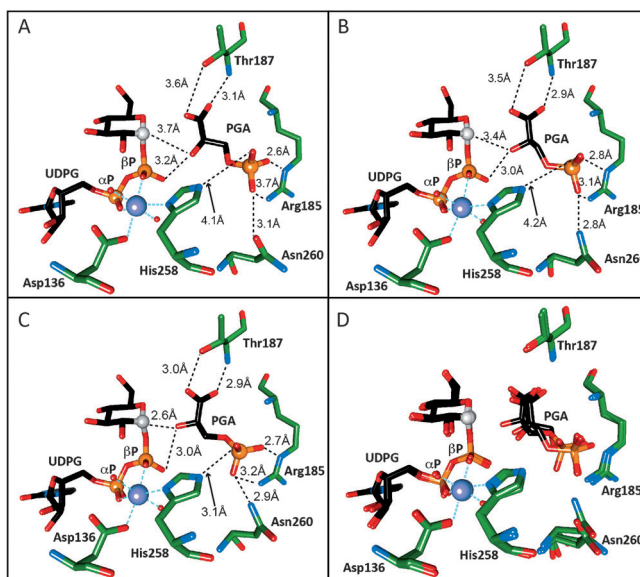


Figure 2. Three snapshots of the reaction center as visualized in the crystal structures of the ternary complexes $\text{GpgS}\cdot\text{Mn}^{2+}\cdot\text{UDP-Glc}\cdot\text{PGA}$ -3 (A; PDB code 4Y9X), $\text{GpgS}\cdot\text{Mn}^{2+}\cdot\text{UDP-Glc}\cdot\text{PGA}$ -2 (B; pre-Michaelis complex, PDB code 4Y6U), and $\text{GpgS}\cdot\text{Mn}^{2+}\cdot\text{UDP-Glc}\cdot\text{PGA}$ -1 (C; Michaelis complex, PDB code 4Y6N). D) Structural comparison of a selected region of the active site in the $\text{GpgS}\cdot\text{Mn}^{2+}\cdot\text{UDP-Glc}\cdot\text{PGA}$ -1, $\text{GpgS}\cdot\text{Mn}^{2+}\cdot\text{UDP-Glc}\cdot\text{PGA}$ -2, and $\text{GpgS}\cdot\text{Mn}^{2+}\cdot\text{UDP-Glc}\cdot\text{PGA}$ -3 complexes.

GpgS is a homodimer, with each monomer displaying a well-defined and positively charged tunnel, which is compatible with the binding of phosphate-containing substrates such as UDP-Glc and PGA (Figure 1B and Figure S4).^[18] This tunnel is shaped in the form of two opposing funnels, separated by a flexible loop that seems to modulate substrate binding and playing a critical role during the catalytic cycle.^[18] Both the UDP-Glc and PGA substrates and the cofactor are clearly visible in the electron density maps, and are located in the center of the tunnel where the Glc transfer reaction takes place (Figure S4). Importantly, close inspection of the active site of GpgS revealed the absence of a putative nucleophile residue that could result in the formation of a glycosyl-enzyme covalent intermediate. Therefore, it is expected that the reaction catalyzed by GpgS would proceed through a front-side substrate-assisted $\text{S}_{\text{N}}\text{i}$ -type mechanism. The first step in such a reaction would be the breaking of the glucosidic $\text{O}_\text{P}\text{--C1'}$ bond, which accounts for

most of the activation energy and is facilitated by a critical stabilizing interaction of the acceptor hydrogen atom O3 of the acceptor PGA with the β -phosphate of the nucleotide sugar. Interestingly, in the first crystal structure (GpgS-Mn²⁺-UDP-Glc-PGA-3, PDB code 4Y9X), the acceptor oxygen atom O3 of PGA is located at a large distance of 3.7 Å from the anomeric carbon C1' of the sugar and 3.2 Å from the O1B atom of the β -phosphate (Figure 2A). In a second crystal structure (GpgS-Mn²⁺-UDP-Glc-PGA-2, PDB code 4Y6U), a pre-Michaelis complex shows the anomeric carbon C1' of the sugar at a position 3.4 Å from the acceptor oxygen atom O3 of PGA. The O1B atom of the β -phosphate is 3.0 Å from the O3 atom of PGA (Figure 2B). In the Michaelis complex (GpgS-Mn²⁺-UDP-Glc-PGA-1, PDB code 4Y6N), the anomeric carbon C1' of the sugar approaches only 2.6 Å from the acceptor oxygen atom O3 of PGA, which in turn hydrogen bonds with the O1B atom of the β -phosphate (Figure 2C,D). The configuration of the active site in the native Michaelis complex of GpgS for the wild type enzyme and with the natural substrates thus provides strong experimental evidence in support of the mechanism described above.

Two additional ternary complexes provide significant insight not only into the binding mode of the sugar donor and acceptor substrates in the active site, but also into the catalytic mechanism of GpgS (Figure 3, Table S1, and Figure S6). The first complex was solved with UDP-Glc, 3-(phosphonoxy)propanoic acid (PPA, an analogue of PGA

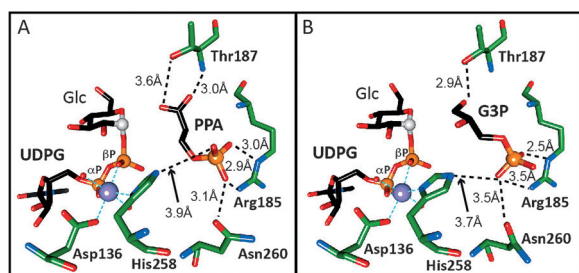


Figure 3. The catalytic site as visualized in the crystal structures of the ternary complexes GpgS-Mn²⁺-UDP-Glc-PPA (A; PDB code 4Y7F) and GpgS-Mn²⁺-UDP-Glc-G3P (B; PDB code 4Y7G).

that lacks the glucose-accepting hydroxy group), and Mn²⁺ as a divalent cation (GpgS-Mn²⁺-UDP-Glc-PPA, PDB code 4Y7F; Figure 3A). We confirmed that the enzyme was unable to transfer a Glc residue to PPA (see the Supporting Information). The carboxyl group of PPA superimposes well with the corresponding moiety of PGA, as observed in the ternary complex GpgS-Mn²⁺-UDP-Glc-PGA-1. However, C2, C3, and the phosphate moiety adopt a different conformation (root-mean-square deviation (r.m.s.d.) of 0.9 Å; Figure 2). As expected, there is no electron density that could indicate the formation of a covalent adduct between the GT and the Glc moiety in the GpgS-Mn²⁺-UDP-Glc-PPA complex. The second complex was solved with UDP-Glc, glycerol 3-phosphate (G3P, an analogue of PGA in which the carboxyl group is replaced by a hydroxy group), and Mn²⁺ as a divalent

cation (GpgS-Mn²⁺-UDP-Glc-G3P PDB code 4Y7G; Figure 3B). The phosphate group of PGA forms hydrogen bonds with the lateral chains of Arg185 and Asn260, as previously visualized in the GpgS-Mn²⁺-UDP-Glc-PGA-1 and GpgS-Mn²⁺-UDP-Glc-PPA complexes. However, the rest of the G3P molecule displays a different structural arrangement (r.m.s.d. of 2.5 Å). Specifically, the oxygen atom O2 of G3P, which is equivalent to the acceptor oxygen atom O3 of PGA, moves away from the Glc moiety to form new electrostatic interactions with the guanidinium group of Arg256 and the lateral chain of His258. The oxygen atom O1 forms a hydrogen bond with the side chain OG1 atom of Thr187 residue (Figure 3B). Altogether the experimental data strongly support the idea of the carboxyl moiety of PGA playing a key role in the generation of a competent reaction center for GpgS.

To further investigate the importance of the carboxyl moiety of PGA, we synthesized a PGA derivative in which the carboxyl group was replaced by amide (PGD; see the Supporting Information). Interestingly, PGD, as with G3P, could not serve as an acceptor for Glc, although it contains the oxygen atom O3 of PGA (the Supporting Information). In addition, despite much effort, we were unable to crystallize GpgS in complex with the PGD derivative, even through soaking or co-crystallization experiments. A plausible explanation is that the carboxyl O2 of PGA forms a strong hydrogen bond with the main-chain amino group of Thr187 in GpgS-Mn²⁺-UDP-Glc-PGA-1. The presence of an amide group in PGD might thus lead to electrostatic repulsion with Thr187, thereby preventing its binding to GpgS.

The experimental native Michaelis complex of GpgS is in good agreement with the predicted Michaelis complexes of lipopolysaccharyl- α -1,4-galactosyltransferase C (LgtC),^[11,17] trehalose-6-phosphate synthase (OtsA),^[15,20] and the recently obtained polypeptide *N*-acetylgalactosaminyltransferase 2, which contains the UDP-GalNAc derivative UDP-5SGalNAc and the truncated incompetent mEA2 peptide STCPA (GalNAc-T2, GalNAc = *N*-acetylgalactosamine; Figure S7).^[16] The LgtC Michaelis complex was modeled based on a crystal structure containing the two substrate analogues UDP 2-deoxy-2'-F-Gal and 4-deoxylactose. The attacking hydroxy group of lactose has the oxygen atom O4 at a distance of 3.1 Å from the anomeric carbon C1' of the donor Gal moiety and 2.7 Å from the glycosidic oxygen atom. Moreover, the O3 of the acceptor lactose also forms a hydrogen bond with the β -phosphate of UDP, thus stabilizing leaving group departure.^[17] The OtsA Michaelis complex was constructed based on its complex with UDP and validoxylamine-6-phosphate (VA6P), a compound that structurally resembles to one of the reaction products, trehalose-6-phosphate. The anomeric carbon C1' of the Glc moiety is 3.0 Å from the O1' of the Glc-6-phosphate acceptor.^[15] In GalNAc-T2, the hydroxy oxygen atom OG1 of the acceptor Thr is 2.5 Å from the anomeric carbon C1' of the GalNAc moiety, and 2.7 and 3.6 Å from the two β -phosphate oxygen atoms of UDP moiety.^[16] In addition, the backbone amide of the acceptor Thr is also hydrogen bonded to the β -phosphate.^[21] Similarly, in GpgS the acceptor oxygen atom O3 of the acceptor PGA is placed 2.6 Å from the anomeric carbon C1' in the Glc residue,

and 2.4 and 3.0 Å from the corresponding β -phosphate oxygen atoms of the UDP moiety. No other interactions are observed between the donor and acceptor substrates in GpgS. Extensive theoretical studies using QM/MM calculation simulations supported the occurrence of the S_N1 'internal return' mechanism in OtsA, LgtC, and GalNAc-T2.^[15–17,21]

We employed molecular dynamics simulations combined with QM(DFT)/MM calculations to further understand the reaction mechanism of GpgS (Figure 4; see Figure S9 and discussion in the Supporting Information for further details). The sugar transfer was modeled by using the reaction coordinate $RC = [d(O_P-C1') - d(O3_{PGA}-C1') - d(HO3_{PGA}-O_P)]$ to drive the system from reactants to products at a QM-

(DFT)/MM level of theory that we have successfully applied in other retaining GTs.^[6,17,21] Two transition states (TS1 and TS2) and a short-lived ion-pair intermediate (IP) connecting them were found (Figure 4 and Table S2), so that an asynchronous mechanism is obtained. As depicted in Figure 4, the reaction starts with the O_P-HO3_{PGA} hydrogen bond getting shorter (by ca. 0.4 Å, $RC = -3.6$ Å). This interaction between the donor and acceptor substrates occurs in all retaining GTs studied to date and seems to be essential in facilitating nucleotide-sugar bond breakage (substrate-assisted catalysis). In TS1, the O_P-C1' distance increases to 2.68 Å, $HO3_{PGA}$ is 1.65 Å from O_P , and the $O3_{PGA}-C1'$ distance shortens to 2.62 Å. Breakage of the UDP-Glc bond results in a positive charge increase of $\Delta q(C1' + H1' + O5') = 0.36$ a.u. at the anomeric center (Table S2). Importantly, the ring conformation changes from a 4C_1 chair in the reactants to a 4E half chair in TS1, with the $C1'-O5'$ distance indicating the development of double-bond character (Table S2). The energy cost to reach TS1 is 21.4 kcal mol⁻¹. After TS1, the energy along the reaction coordinate decreases by approximately 2 kcal mol⁻¹, and a short-lived oxocarbenium intermediate is formed (sugar ring conformation between 4E and 4H_5). In this IP, the glucosidic bond is definitely broken (the O_P-C1' distance is now 3.20 Å), whereas the $HO3_{PGA}-O3_{PGA}$ and $C1'-O5'$ distances remain practically invariant with respect to TS1. The attacking $O3_{PGA}$ atom gets 0.3 Å closer to $C1'$. The energy of the optimized IP is 0.6 kcal mol⁻¹ lower than that of TS1. From the IP, acceptor attack takes place through TS2, in which the $C1'-O3_{PGA}$ and $HO3_{PGA}-O_P$ distances are 2.26 Å and 1.56 Å, respectively. TS2 lies 21.8 kcal mol⁻¹ above the Michaelis complex and 0.5 kcal mol⁻¹ above the IP. Therefore, most of the overall energy barrier for the transfer reaction to take place is due to glucosidic O_P-C1' bond dissociation. These energies indicate that the IP could be a very short-lived species with no time to thermally equilibrate. The calculated rate-limiting energy barrier (21.8 kcal mol⁻¹) is in reasonable agreement with the experimentally derived phenomenological free energy of activation of 17.5 kcal mol⁻¹ (derived from a k_{cat} value of 800 min⁻¹; see the Supporting Information), thus supporting the idea that GpgS follows a front-side attack mechanism.

Intriguingly, the active sites of a few GTs display a carboxylate residue, which allows these enzymes to follow a double-displacement reaction,^[6,7,9] whereas most of retaining GTs, in the absence of such nucleophile, seem to follow a front-side mechanism. We propose that the two mechanisms might represent different manners of stabilizing the oxocarbenium ion like species that forms upon cleavage of the donor sugar-phosphate bond. In GpgS, the electrostatic potential at the reaction center can stabilize the oxocarbenium ion like intermediate for a very short period of time, thereby allowing the active site to reorganize and the oxocarbenium ion species and acceptor to move towards each other. By contrast, in the α -1,3-galactosyltransferase GTB^[22] or the *N*-acetyllactosaminide α -1,3-galactosyl transferase α 3GalT,^[23] the oxocarbenium ion like transition state is stabilized by the formation of a covalent bond with the nucleophile residue present in these enzymes. Thus, as we

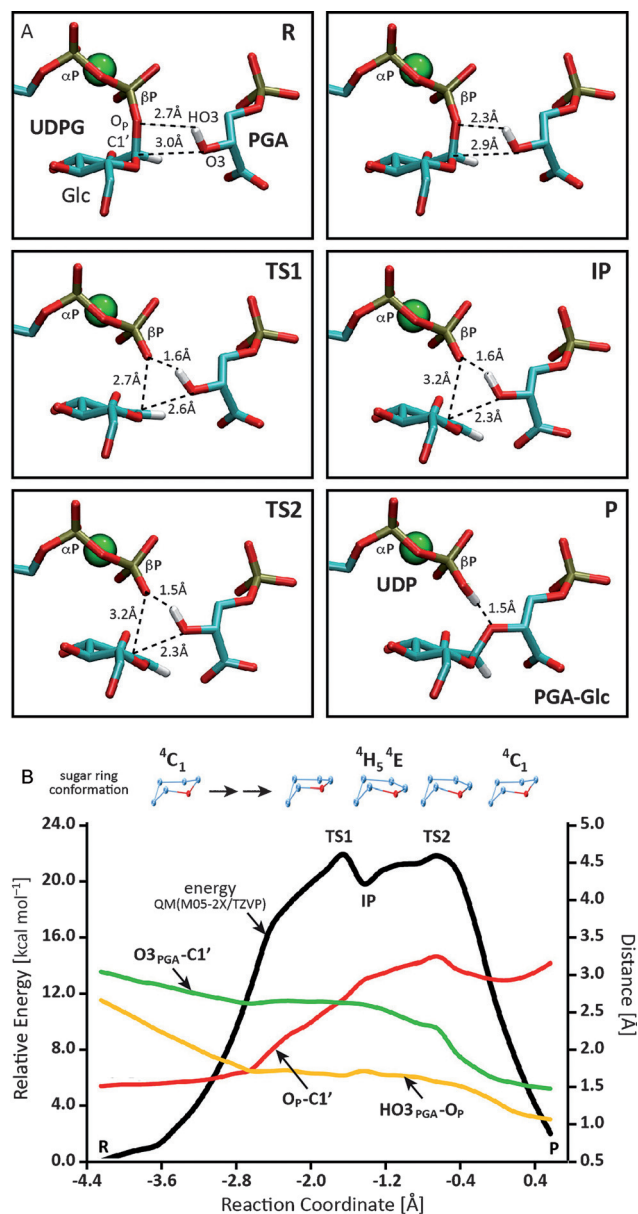


Figure 4. A) Atomic rearrangement along the reaction pathway in GpgS: optimized reactants (R), structure at $RC = -3.6$ Å, transition state 1 (TS1), ion-pair intermediate (IP), transition state 2 (TS2), and products (P). B) Structural and energetic changes along the reaction coordinate.

initially proposed,^[7] the two modes of operation could be considered as variations of a common mechanism: a two-step reaction via oxocarbenium ion like transition states that flank an intermediate, either an oxocarbenium ion or a covalent glycosyl-enzyme intermediate, depending of the active-site configuration.

Keywords: enzyme catalysis · enzymes · glycosyltransferases · reaction mechanisms · structure elucidation

How to cite: *Angew. Chem. Int. Ed.* **2015**, *54*, 9898–9902
Angew. Chem. **2015**, *127*, 10036–10040

- [1] L. L. Lairson, B. Henrissat, G. J. Davies, S. G. Withers, *Annu. Rev. Biochem.* **2008**, *77*, 521–555.
- [2] D. Albesa-Jové, D. Giganti, M. Jackson, P. M. Alzari, M. E. Guerin, *Glycobiology* **2014**, *24*, 108–124.
- [3] A. Varki, *Essentials of Glycobiology*, 2nd ed. (Eds.: A. Varki, R. Cummings, J. Esko, H. Freeze, P. Stanley, C. R. Bertozzi, G. Hart, M. E. Etzler) Cold Spring Harbor Laboratory Press, Cold Spring Harbor, NY, **2009**.
- [4] A. Monegal, A. Planas, *J. Am. Chem. Soc.* **2006**, *128*, 16030–16031.
- [5] H. Gómez, J. M. Lluch, L. Masgrau, *Carbohydr. Res.* **2012**, *356*, 204–208.
- [6] H. Gómez, J. M. Lluch, L. Masgrau, *J. Am. Chem. Soc.* **2013**, *135*, 7053–7063.
- [7] V. Rojas-Cervellera, A. Ardèvol, M. Boero, A. Planas, C. Rovira, *Chem. Eur. J.* **2013**, *19*, 14018–14023.
- [8] N. Soya, Y. Fang, M. M. Palcic, J. S. Klassen, *Glycobiology* **2011**, *21*, 547–552.
- [9] A. Bobovská, I. Tvaroška, J. Kóňa, *Glycobiology* **2015**, *25*, 3–7.
- [10] M. L. Sinnott, W. P. Jencks, *J. Am. Chem. Soc.* **1980**, *102*, 2026–2032.
- [11] K. Persson, H. D. Ly, M. Dieckelmann, W. W. Wakarchuk, S. G. Withers, N. C. Strynadka, *Nat. Struct. Biol.* **2001**, *8*, 166–175.
- [12] R. P. Gibson, J. P. Turkenburg, S. J. Charnock, R. Lloyd, G. J. Davies, *Chem. Biol.* **2002**, *9*, 1337–1346.
- [13] S. S. Lee, S. Y. Hong, J. C. Errey, A. Izumi, G. J. Davies, B. G. Davis, *Nat. Chem. Biol.* **2011**, *7*, 631–638.
- [14] A. Bobovská, I. Tvaroška, J. Kóňa, *Org. Biomol. Chem.* **2014**, *12*, 4201–4210.
- [15] A. Ardèvol, C. Rovira, *Angew. Chem. Int. Ed.* **2011**, *50*, 10897–10901; *Angew. Chem.* **2011**, *123*, 11089–11093.
- [16] E. Lira-Navarrete, J. Iglesias-Fernández, W. F. Zandberg, I. Compañón, Y. Kong, F. Corzana, B. M. Pinto, H. Clausen, J. M. Peregrina, D. J. Vocadlo, C. Rovira, R. Hurtado-Guerrero, *Angew. Chem. Int. Ed.* **2014**, *53*, 8206–8210; *Angew. Chem.* **2014**, *126*, 8345–8349.
- [17] H. Gómez, I. Polyak, W. Thiel, J. M. Lluch, L. Masgrau, *J. Am. Chem. Soc.* **2012**, *134*, 4743–4752.
- [18] S. Urresti, D. Albesa-Jové, F. Schaeffer, H. T. Pham, D. Kaur, P. Gest, M. J. van der Woerd, A. Carreras-González, S. López-Fernández, P. M. Alzari, P. J. Brennan, M. Jackson, M. E. Guerin, *J. Biol. Chem.* **2012**, *287*, 24649–24661.
- [19] M. Jackson, P. J. Brennan, *J. Biol. Chem.* **2009**, *284*, 1949–1953.
- [20] J. C. Errey, S. S. Lee, R. P. Gibson, C. Martinez Fleites, C. S. Barry, P. M. Jung, A. C. O'Sullivan, B. G. Davis, G. J. Davies, *Angew. Chem. Int. Ed.* **2010**, *49*, 1234–1237; *Angew. Chem.* **2010**, *122*, 1256–1259.
- [21] H. Gómez, R. Rojas, D. Patel, L. A. Tabak, J. M. Lluch, L. Masgrau, *Org. Biomol. Chem.* **2014**, *12*, 2645–2655.
- [22] J. A. Alfaro, R. B. Zheng, M. Persson, J. A. Letts, R. Polakowski, Y. Bai, S. N. Borisova, N. O. Seto, T. L. Lowary, M. M. Palcic, S. V. Evans, *J. Biol. Chem.* **2008**, *283*, 10097–10108.
- [23] E. Boix, Y. Zhang, G. J. Swaminathan, K. Brew, K. R. Acharya, *J. Biol. Chem.* **2002**, *277*, 28310–28318.

Received: May 21, 2015

Published online: July 1, 2015